J. Am. Ceram. Soc., 94 [9] 2906–2911 (2011)
DOI: 10.1111/j.1551-2916.2011.04691.x

journal

Effect of Bromine on NaF Crystallization in Photo-Thermo-Refractive Glass

G.P. Souza,[‡,†] V.M. Fokin,[§] C.A. Baptista,[‡] E.D. Zanotto,[‡] J. Lumeau,[¶] L. Glebova,[¶] and L.B. Glebov,[¶]

[‡]Vitreous Materials Lab (LaMaV), Department of Materials Engineering (DEMa), Federal University of São Carlos, 13565-905, São Carlos, SP, Brazil

[§]Vavilov State Optical Institute, ul. Babushkina, 36-1, 193 171, St. Petersburg, Russia

[¶]CREOL/The College of Optics and Photonics, University of Central Florida, 4000 Central Florida Blvd., Orlando, Florida, 32816 USA

Photo-thermo-refractive (PTR) glass is a Na_2O–K_2O–ZnO–Al_2O_3–SiO_2 silicate optical glass which also contains fluorine, a small amount of bromine, and dopants that yield photo-sensitivity in the UV range. PTR glass undergoes crystallization of NaF nanocrystals after UV-exposure followed by thermal treatment, resulting in permanent refractive index change. In this study, where we explore only the thermally activated transformations in the UV-unexposed glass, we show that bromine decreases the solubility of NaF, i.e., increases the super-saturation of NaF thus increasing the thermodynamic driving force for crystallization. This feature causes a decrease in the maximum volume fraction of crystallized NaF with decreasing bromine content in the parent glass. The evolution of the glass transition temperature, T_g, with increasing isothermal treatment time revealed a minimum resulted from interplay between two concurring processes, liquid–liquid phase separation that led to decrease in T_g, and Br-controlled NaF crystallization that acted in the opposite direction. In glasses with lower bromine content, fewer and larger crystals appeared and a surface-initiated crystallization was dominant. A surface layer of F-depleted glass imprinted residual macro-stresses, which were not alleviated by annealing.

I. Introduction

PHOTO-THERMO-REFRACTIVE (PTR) glass is a photo-sensitive Na_2O–K_2O–ZnO–Al_2O_3–SiO_2 glass doped with cations Ce, Ag, Sb, and Sn, and anions F and Br. This glass undergoes crystallization of less than 1 vol% NaF nanocrystals after UV-exposure followed by thermal processing which promotes permanent refractive index change.[1,2] The fact that after thermal processing the refractive index of the UV-exposed regions of the glass differs from that of the UV-unexposed regions, allows PTR glass to serve as a medium for highly efficient volume holographic optical elements (HOEs).[3] Typical commercial applications are in: laser beam combiners, deflectors, splitters, and attenuators; selectors of transverse and longitudinal modes in laser resonators; and narrow-band spectral filters.[4] To achieve high efficiency, HOEs must be highly transparent (losses $< 10^{-3}$ cm^{-1}) within the range of wavelengths of their application (350–2700 nm). Thus, absorption and scattering must be prevented. This can only be achieved through the complete understanding of the physical and chemical transformations PTR glass undergoes during photo-thermal processing.

A tentative description of the photo-induced, thermally activated crystallization of this type of glass was proposed 60 years ago[5]: (i) photo-oxidation of Ce^{3+} and formation of atomic silver during exposure to UV ($Ag^+ + Ce^{3+} + h\nu \rightarrow Ag^0 + Ce^{4+}$), (ii) atomic silver clustering during a first thermal treatment at 450°–500°C, and (iii) heterogeneous nucleation and growth of NaF nanocrystals on further heating. However, recent studies demonstrated that bromine—which does not appear in the above simplified mechanism—plays a key role in the crystallization of NaF. Cardinal *et al.*[6] reported X-ray diffraction peaks of NaBr in UV-exposed PTR glass after 1 h isothermal treatment at temperatures between 580° and 780°C. However, no explanation of the role of bromine in the crystallization process was provided. It was later shown that decreasing the bromine content in the parent glass severely hindered NaF crystallization.[7] This was revealed by following the evolution of a differential scanning calorimetry (DSC) exothermic event, assigned as NaF crystallization, for PTR glass samples with various bromine contents. In the same study, optical spectroscopy indicated that AgBr could be one of the phases formed during crystallization of PTR glass. This was further investigated in Reference [8], where it was shown that an absorption band at ~530 nm, possibly due to AgBr, appeared during cooling of the UV-exposed PTR glass. In spite of the experimental observation that Br is essential in the precipitation of crystalline NaF, the actual role of bromine in the crystallization path of PTR glass, as well as the fundamental mechanism of photo-induced crystallization, are still debatable. This is why several recent studies were directed to the fundamental understanding of NaF crystallization in PTR glass that has not been exposed to UV, thus eliminating the photo-induced aspect of the nucleation process. Throughout this text we refer to the crystallization of the UV-unexposed glass as *thermal crystallization*, realizing that crystallization of all glasses is a thermally activated process and that the difference between crystallization of UV-unexposed and UV-exposed PTR glasses refers only to the intricate nucleation mechanism. This should be considered though as a first approximation for photo-induced crystallization study.

Thermal crystallization (from now on referred as *crystallization*) of NaF in PTR glass was shown to change the composition of the residual glass as fluorine and sodium go into crystals, creating a marked diffusion zone around NaF crystals.[9] The maximum amount of NaF that can crystallize at a given temperature depends on both NaF solubility and its original content in the parent glass. For a given (parent) glass composition, the maximum volume fraction of crystallized NaF increases with decreasing the heat treatment temperature, due to a decrease in NaF solubility.[10] Decreasing

L. Pinckney—contributing editor

Manuscript No. 29384. Received February 27, 2011; approved May 25, 2011.
This work was supported by DARPA ADHELS program, contract HR-0011-06-1-0010. EDZ acknowledges Brazilian funding agencies CNPq and FAPESP contract no. 2007/08179-9. GPS and VMF acknowledge FAPESP, contracts no. 2008/02645-0 and 2008/00475-0, respectively.
[†]Author to whom correspondence should be addressed. e-mail: gparente003@hotmail.com

NaF dissolved in the residual glass due to NaF crystallization increases the glass transition temperature (T_g). In the present study, crystallization of NaF in PTR glasses containing various bromine contents is studied along with the evolution of T_g measured by DSC. Complementary techniques such as optical microscopy and X-ray diffraction are used to correlate those findings with microstructural and phase evolution.

II. Experimental Procedure

The PTR glasses with composition (by synthesis) $15Na_2O$–$5ZnO$–$4Al_2O_3$–$70SiO_2$–$5NaF$–xKBr–$0.01Ag_2O$–$0.01CeO$–$0.01SnO_2$–$0.03Sb_2O_3$ (mol%), x varied from 0 to 1 mol% with 0.25 mol% steps, were melted at 1460°C for 5 h, annealed at 460°C for 2 h, and cooled to room temperature at 0.1 K/min. The glasses were not submitted to UV radiation exposure i.e., the glass samples are UV-unexposed. Further details on the glass melting and homogeneity, as well as detailed procedure for estimating the bromine content in the glass melts are described in Reference [7]. Glass melts were denoted according to the bromine content as Br0, Br25, Br50, Br75, and Br100 (Table I). Actual concentration of bromine was approximately two times lower than that calculated as per synthesis, resulted from the high volatility of Br-containing compounds, as investigated by SIMS in Reference [7]. Isothermal treatments at 600°C were carried out in a vertical electric box furnace. Samples ~3 mm × 3 mm × 3 mm were dropped into the furnace previously stabilized at 600°C. After a given period of time at this temperature, the samples were quenched in air to room temperature. Estimated heating and cooling rates of glass samples were ~500 K/min. A Netzsch 404 differential scanning calorimeter (DSC) (Netzsch, Selb, Bavaria, Germany) was used to record T_g of the samples before and after thermal treatments. DSC curves were recorded from room temperature to 650°C at 10 K/min. Samples were run in a platinum crucible against an empty platinum crucible, used as reference.

The equilibrium volume fraction of the crystallized phase (α_{eq}) NaF was measured by quantitative X-ray diffraction (XRD) analysis.[11] XRD measurements were carried out on powdered samples using a Siemens D5005 X-ray diffractometer (Siemens, Munich, Germany) operating at 40 mA and 40 kV. Cu$K\alpha$ (1.5406 Å) was used as incident radiation to scan samples from $36° \leq 2\theta \leq 41°$ at a scanning speed of 0.6°/min. The area S_{200} of the strongest NaF diffraction peak (200) was measured for the five glasses heat-treated at 600°C for 24 h. Areas were converted into α_{eq} via a calibration plot S_{200}-α obtained for (0, 5, 10, and 15 vol% NaF) powder mixtures of untreated PTR glass with pure crystalline NaF, as described in Reference [10]. The volume fraction of crystallized NaF was then recalculated into weight percent using glass and crystal densities.

A Leica DMRX optical microscope (Leica, Wetzlar, Germany) coupled to a Leica DFC490 CCD camera was used in both transmitted and reflected light modes. For reflected light optical microscopy of thermally treated and cross-sectioned samples, these were cut, mounted in Epoxy resin, ground, and polished. Etching in a 2 vol% HF aqueous solution for 2 min enhanced the topographic contrast. For transmitted light microscopy, samples of cubic (~3 mm × 3 mm × 3 mm) shape were prepared to reveal details of volume and surface-initiated crystallization. In addition, polarized light was used to highlight residual stresses due to compositional variations in glass samples between the surface layer and the bulk (this effect is detailed in the Discussion section). For the cross-polarized transmitted light microscopy experiments, we removed all compensators and set the analyzer at 90° and the polarizer at 0°. Since all studied samples were observed under the same conditions we could perform a comparative analysis.

Table I. Bromine Content in Glasses by Synthesis

Glass	Bromine content (at.%)
Br0	0
Br25	0.08
Br50	0.17
Br75	0.25
Br100	0.34

III. Results

The glass transition temperature (T_g) as a function of heat treatment time at 600°C, of glass samples with various bromine contents, is shown in Fig. 1. One can see that T_g of all original glasses, from here onwards denoted T_g^0, is similar (within a ~5 K range), with no clear trend as for varying as a function of Br content. For the Br100 glass, which has the maximum bromine content (Table I), T_g swiftly shifted to higher temperatures with increasing the heat treatment duration. NaF crystallization leads to depletion of the glassy matrix in sodium and fluorine, hence increasing T_g. Saturation of T_g at the level of $T_{g/s}$ = 509°C is reached after ~2 h heat treatment at 600°C, indicating that all NaF that could crystallize at that temperature has precipitated and is in equilibrium with the Na and F ions that remain in solution, according to the NaF solubility. It should be noted that the kinetics of T_g change is dramatically different in glasses with decreased bromine content. The same heat treatment applied to Br75 caused a ~10 K decrease of T_g within the first 1 h of heat treatment before starting a gradual rise, and finally reaching its saturation value ($T_{g/s}$ = 504°C) which is slightly lower than that for Br100. Further decrease of the bromine content in PTR glass, as from Br75 to Br50, led to a larger decrease in T_g in the first stages of thermal treatment before the gradual climb toward $T_{g/s}$. Compared to Br75, the Br50 glass reached $T_{g/s}$ earlier, but $T_{g/s}$ for Br50 is even lower than that for the untreated glass (T_g^0). The same trend was observed for Br25, where the time needed to reach $T_{g/s}$ was comparable to that for Br50, and $T_{g/s}$ was lower than T_g^0. In the case of Br0 (i.e., the glass without bromine), T_g underwent the same drop of ~10 K observed for Br75, Br50, and Br25. However, in the case of Br0, T_g did not recover from its initial drop. The minimum in the dependence of T_g on duration of thermal treatment was described in Reference [10] as resulting from the interplay between concurrent liquid–liquid phase separation (LLPS) and NaF crystallization. Absence of NaF crystallization in the Br0 glass eliminates this minimum, and leaves only the T_g drop followed by a plateau. XRD trace for Br0 heat-treated at 600°C for 6 h is shown in Fig. 2. No clearly defined crystalline peaks are present.

Decrease in $T_{g/s}$ with decreasing the bromine content can be better visualized in Fig. 1(f) where all curves are compared in the same T_g vs *time* plot. To have a better idea about the effect of bromine on NaF crystallization on the basis of T_g change, the difference $T_{g/s}-T_g^0$ was plotted against the bromine content in Fig. 3. Positive values of $T_{g/s}-T_g^0$ mean that after the temperature drop, the T_g change due to NaF crystallization reached a higher value of T_g compared to the untreated glass (T_g^0). The higher the bromine content in PTR glass, the higher is $T_{g/s}-T_g^0$. For glasses with bromine content lower than 0.25 at.%, $T_{g/s}$ was below T_g^0 since the effect of LLPS was stronger than that of NaF crystallization. Figure 4 shows α_{eq}, the equilibrium volume fraction of crystallized NaF at T = 600°C, plotted as a function of bromine content of the parent glasses. Correlation between the evolution of α_{eq} and $T_{g/s}-T_g^0$ with the bromine content can be observed by comparing Figs. 3 and 4. This confirms the crucial role of NaF crystallization in increasing T_g of the glass. The solubility of NaF in wt% for

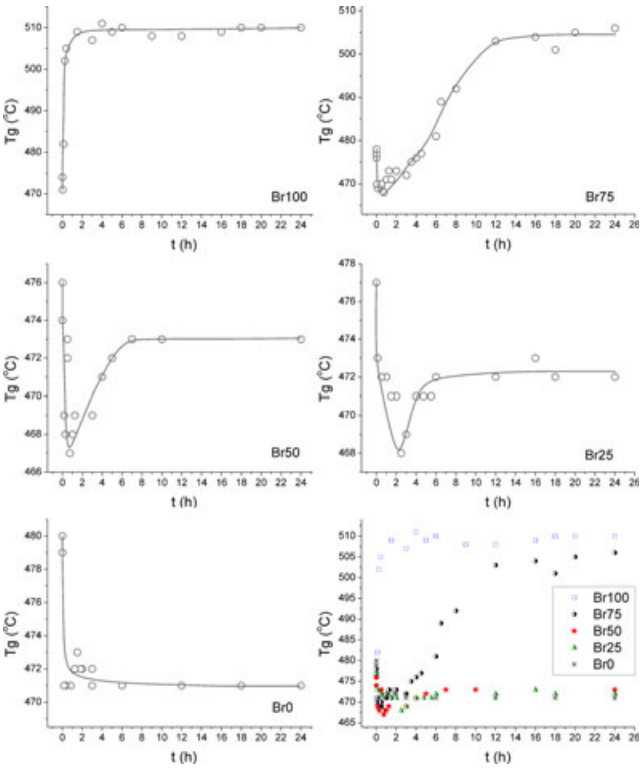

Fig. 1. Dependence of T_g of the glasses with different bromine content on isothermal treatment duration at 600°C. Scales of vertical axes are different.

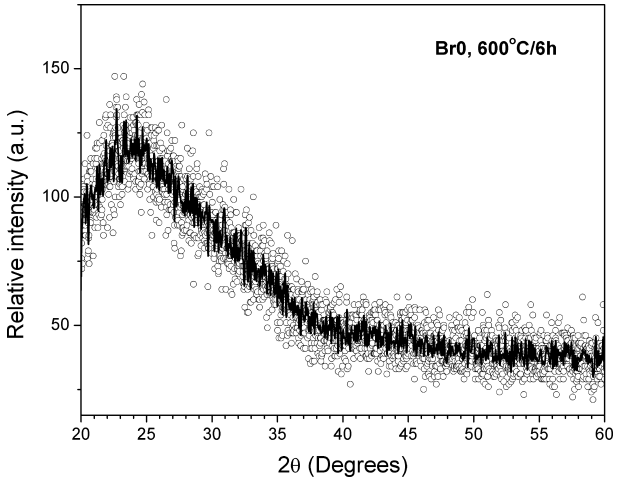

Fig. 2. XRD trace of the Br0 glass heat-treated at 600°C for 6 h. Smoothing of raw data is represented by a solid line.

T = 600°C was calculated from the equilibrium fraction of NaF crystals, α_{eq}, in the following way:

$$\chi_{NaF} = \frac{(C_{NaF}100 - 100\alpha_{eq})}{(100 - \alpha_{eq})} \quad (1)$$

Dependence of NaF solubility at T = 600°C on the bromine content in the parent glass is shown in Fig. 4. One can see dramatic drop of solubility for glasses with bromine concentration exceeding 0.2 at.% (by synthesis).

The microstructural variation while increasing the bromine content in PTR glass thermally treated at 600°C for 24 h revealed by reflected light optical microscopy is shown in

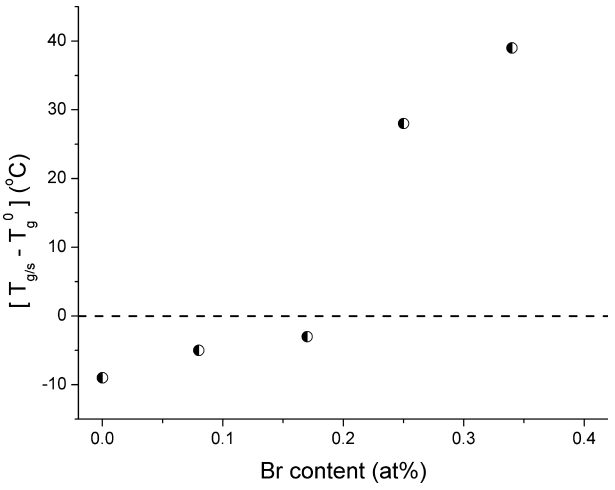

Fig. 3. Dependence of difference between $T_{g/s}$ and T_g^0 on bromine concentration in glasses.

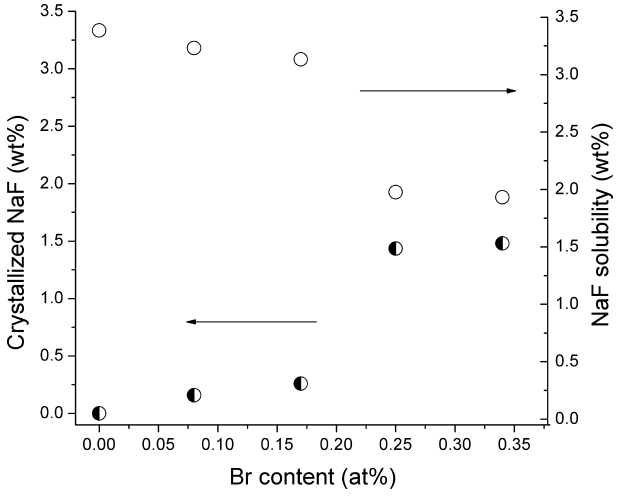

Fig. 4. Dependence of NaF crystalline fraction in saturation, and of solubility of NaF at T = 600°C, on bromine concentration.

Fig. 5. NaF crystals in the Br100 glass are more numerous and smaller than those in glasses with lower bromine content. With a decrease in the bromine content, the decrease in crystallized fraction of NaF (α_{eq}) (as shown in Fig. 4) is accompanied by a decrease in crystal number density. The fewer crystals (with decreasing the bromine content) are progressively larger, with a distinct dendritic morphology. For Br100, average crystal size is ~2 μm, whereas for Br75 it is ~30 μm, and for Br50 it is ~75 μm. For the Br50 glass [Fig. 5(c)], only the black areas of the dendrite shown are in focus with the surface of the polished and etched sample. In this case, and also for Br25 and Br0, the glass samples are fairly transparent to visible light. Crystals are not visible in cross-sectioned/polished samples of Br0 (as anticipated by XRD, Fig. 2), although very few, large crystals were observed in Br25 (more likely to be visible in transmitted light mode). A detailed area of cross-sectioned sample from Br75, polished and etched with HF, is shown in Fig. 5(f), where dendrites can be clearly seen surrounded by a finer structure [boxed in Fig. 5(f)]. Such fine structure was reported in References [9–10] as droplets of a liquid–liquid phase separated glass. It is worth mentioning that such fine structure is also present in Br100, but the scale of size of the amorphous droplets is very similar to that of the NaF crystals, thus it is difficult to visualize each of them separately. With decreasing bromine content and NaF crystallization,

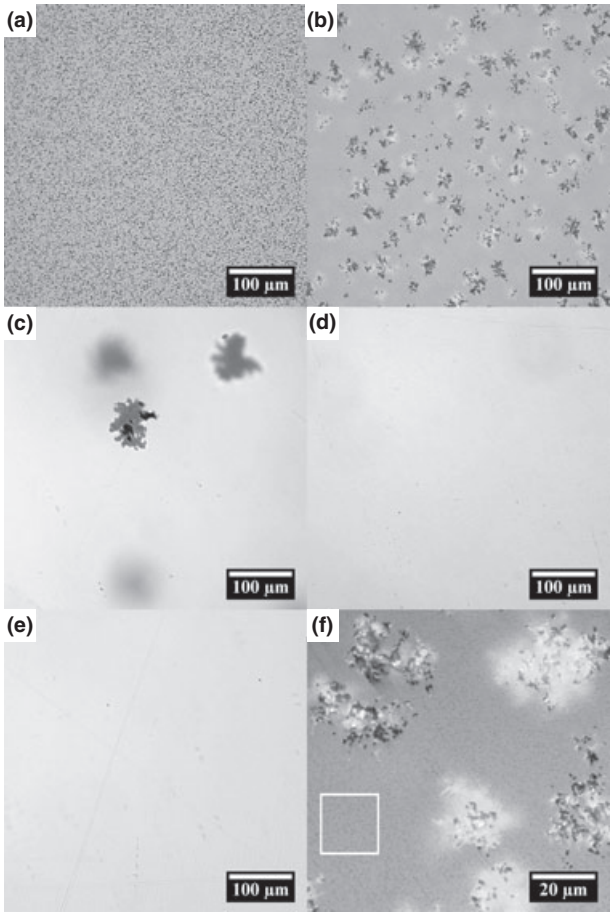

Fig. 5. Reflected light optical micrographs of glass samples with different bromine contents: Br100 (a), Br75 (b, f), Br50 (c), Br25 (d), and Br0 (e); heat-treated at 600°C for 24 h.

the LLPS structure gradually disappears until nothing can be seen for Br0, at least under the resolution limit of the optical microscope. LLPS can become finer as a result of compositional changes in the glass, which may happen in the present case. Moreover, the T_g drop was observed even for the samples where droplets are not clearly seen, indicating the occurrence of LLPS. Therefore, the supposed disappearance of fine (LLPS) structure could be rather a change in the size and morphology of the structure to be less discernible by optical microscopy.

The effect of bromine content in the parent glass on the microstructure of the glass thermally treated at 600°C for 24 h, revealed by transmitted light optical microscopy, is shown in Fig. 6. For each glass, cubic (~3 mm × 3 mm × 3 mm) samples with flat surfaces were heat-treated at 600°C for 24 h. Those samples were cross-sectioned parallel to one of the faces (final thickness ~1.5 mm) and polished (on both sides) for optical microscopy observation. The Br100 glass is opaque to the transmitted (visible) light used, as shown in Fig. 6(a), due to the large number density of (~2 μm) NaF crystals. However, a ~40 μm thick surface layer appeared (arrowed). Such layer is transparent, and encapsulates the entire (~3 mm × 3 mm × 3 mm) cube. According to previous studies[9,12] some fluorine escapes during the course of a heat treatment. In the present case, depletion in fluorine prevented NaF crystallization, forming a non-crystallized cap over the glass sample. A similar picture was found for the Br75 glass (not shown here), with a surface layer depleted of NaF crystals.

For the Br50 glass, a different phenomenon has occurred. The lower bromine content compared to that for the Br100 glass decreased the crystallization level of NaF. Fewer crystals appeared, as discussed for Fig. 5. Those crystals are rather large and have a dendritic morphology. It is interesting to note, though, that most crystals in Br50 are located near the cube's faces. Such crystallization has initiated near the surface of the cube, and progressed (~200 μm) through the bulk. Since Fig. 6(b) gives a misleading idea about the concentration of branches initiated near the faces of the cube, which appears to be very high by looking at the edges of the sample, a top-view perspective of the surface layer of crystallized NaF is shown in Fig. 6(c). The idea was to remove, for instance, the top surface layer of the cube so that one could see through the bulk of the glass until the bottom layer of the cube. By focusing on the opposite (virgin) face of the sample, it becomes clear that branches of NaF do not form a continuous layer. This might be due to the competition for Na and F ions from the glass, particularly the scarce fluorine, in good agreement with the concept of diffusion zones in this system.[9] In the Br25 glass, crystals were fewer and larger than in Br50 [Fig. 6(d)]. A very large crystal with a vermicular morphology appeared in the volume of the cube [shown out of focus in Fig. 6(d)]. A crystallized layer also appeared, but thinner than that in the Br50 glass. Crystals were not observed in the volume of the Br0 glass, and crystallization near the surface of the glass cube was negligible.

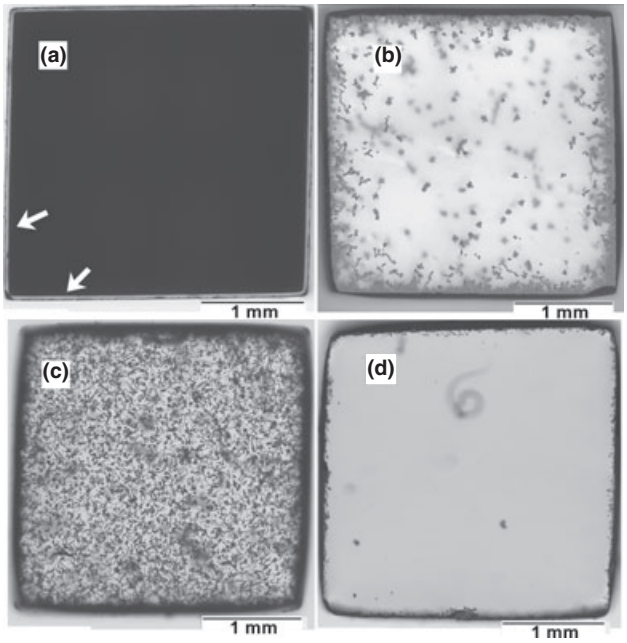

Fig. 6. Transmitted light (a, c–d) and reflected light (b) optical micrographs of glass samples with various bromine contents: Br100 (a), Br50 (b–c), and Br25 (d); heat-treated at 600°C for 24 h. Samples of cubic (~3 mm × 3 mm × 3 mm) shape were cross-sectioned to reveal both volume and surface crystallization. The Br50 glass in (c) had only one of its faces removed, and a top-view of the opposite virgin face is shown in focus.

IV. Discussion

Increase in T_g of studied glasses with an increase in the heat treatment time at 600°C was shown to be faster for Br100 than for melts containing lower bromine content. The low solubility of NaF for that melt increased the super-saturation leading to marked nucleation of NaF crystals, as shown by optical microscopy (Fig. 5), since super-saturation determines the thermodynamic driving force for crystallization. In particular, crystal nucleation depends exponentially on the thermodynamic driving force, and hence on super-saturation.[13] The simultaneous growth of a large number of crystals allowed for swift depletion of fluorine from the glass, yielding fast increase of T_g. The level of saturation of T_g attained by the Br100 glass is only slightly higher than that

for Br75. Nevertheless, this difference results in a strong decrease in the number of NaF crystals in the Br75 glass, while the average crystal size was increased. The variation of T_g reflects compositional change of the residual glass caused by crystallization of NaF. When T_g reaches a constant value, the residual glass comes to equilibrium with the crystalline phase, i.e., the liquid is saturated with NaF. A lower solubility corresponds to a higher maximum value of T_g (after heat treatment), and hence higher equilibrium volume fraction of the crystalline phase. Thus, since the NaF content is the same in all glasses, one can conclude that the solubility of NaF in the Br75 glass is higher than that in the Br100 glass.

The level of $T_{g/s}$ in T_g vs *time* plots progressively drops with decrease in bromine content in the parent glass due to a decrease of equilibrium fraction of NaF α_{eq} (Figs. 3–4). Moreover, within the compositional interval ~0.17–0.25 at.% of bromine a sharp drop in solubility of NaF occurs, resulting in sharp increase of super-saturation of NaF. This finding is corroborated by the dramatic increase in crystal number density with increasing bromine content (Figs. 5 and 6). Different from the nucleation rate, the crystal growth rate depends on the thermodynamic driving force in a weaker manner.[13] The effect of the increase of residual glass viscosity during NaF crystallization on the kinetics of the overall crystallization should be also taken into account. The higher the bromine content the lower the amount of NaF dissolved in the residual glass, and the higher the viscosity. Also, despite the decrease in the equilibrium fraction of crystallized NaF (α_{eq}) with decreasing the bromine content, the average crystal size increases due to strong decrease in the crystal number density. It should also be recalled that some NaBr is crystallized along with NaF,[6–9] thus decreasing the bromine content in the residual glass and increasing the solubility of NaF. This is thought to be a small effect as the crystallized NaBr content is minor. Thus, it is clear that the effect of bromine on the crystallization of NaF in PTR glass encompasses a wide range of inter-related processes. However, the equilibrium fraction of crystalline NaF depends only on the NaF content in the parent glass and its solubility, which strongly increases with decrease in the bromine content.

Along with crystallization of NaF, PTR glasses develop LLPS.[14] This experimental fact is not surprising since the main components of these glasses are sodium and silicon oxides. Liquid–liquid phase separated PTR glass has a droplet structure. Since the droplets are rich in silica, the resulting glass matrix becomes progressively richer in modifier cations, weakening the glass network and yielding a lower T_g. As opposed to LLPS, concurrent crystallization of NaF removes Na and F from the glass matrix and hence increases T_g. The interplay between LLPS and crystallization processes can result in a minimum on the T_g vs *time* plot (Fig. 3). As the crystallization process is suppressed by decreasing the bromine content, the corresponding increase of the T_g is weakened, the minimum becomes weaker and is transformed into a drop of T_g followed by a plateau, where the crystallization process becomes negligible i.e., only the effect of LLPS is visible. However, while LLPS was observed by microcopy in glasses with high bromine content, no similar LLPS structure was observed for the Br0 glass after the same heat treatment. The LLPS structure in Br0 is possibly much finer and not readily visible by the methods employed in this study. It is also known that fluorine strongly affects the LLPS in sodium silicate glasses.[15] It means that bromine may affect the LLPS process via change of α_{eq} and hence of fluorine content in residual glass. Appearance of LLPS in glasses with low bromine concentration requires additional study.

It is clear that thermal treatment of a glass which contains volatile components such as bromine and fluorine causes depletion of those components in the surface layers of the glass sample. The formation of two neighboring glasses (i.e., the bulk glass enfolded by the modified glassy envelope) with different physical properties (e.g., coefficient of thermal expansion and viscosity) generates stresses on cooling to room temperature. The F-depleted glassy envelope is expected to have a lower coefficient of thermal expansion than that of the bulk glass. The thermal expansion mismatch between the two glass phases after freezing (i.e., below T_g) should be small, since their compositional difference is also small. It is also worth noting that part of the fluorine and a small fraction of the sodium turn into crystals upon heat treatment. The F-depleted glassy envelope has higher T_g and viscosity, and thus reaches the glass transition stage earlier than the bulk glass (on cooling). Consequently, the liquid bulk glass pulls the solid glassy envelope into tension during cooling, giving rise to residual stresses. To qualitatively reveal residual stresses, a cube from the Br50 glass was heat-treated at 600°C for 5 min, and quenched (in air) to room temperature. As shown in Fig. 7(a), residual stresses are revealed by cross-polarized transmitted light microscopy (regions near the edges of the cube, like the ones arrowed). In this case, no (or only negligible) crystallization took place, and the stresses were formed on quenching the glass due to the gradient of cooling rate between the bulk and the surface of the sample. The same sample heat-treated at 600°C for 5 min and quenched to room temperature was also annealed, in a second heat treatment, by cooling to room temperature from ~470°C at 1 K/min. As one can observe in Fig. 7(b), the stress-induced birefringence contrast is largely unnoticeable, giving evidence of stress relief.

On the other hand, heat-treating another cubic sample of the same Br50 glass at 600°C for 24 h yields NaF crystallization predominantly near the surface of sample [Figs. 6(b)–(c)], which changes the glass chemistry in that region. Under a quenching regime, stress-induced birefringence is clearly shown in Fig. 7(c). However, annealing the sample does not release the stresses as in the case of the sample initially heat-treated for 5 min [Figs. 6(a)–(b)]. This is shown in Fig. 7(d), where the birefringence pattern is identical to that of the same sample, but quenched [not annealed, Fig. 7(c)]. In this sample, the presence of two different glasses (i.e., the partially crystallized bulk glass and the modified glassy surface layer, or "envelope") produced residual stresses which could not be alleviated by annealing. Such stresses are permanently imprinted in the glass cube of heat-treated Br50.

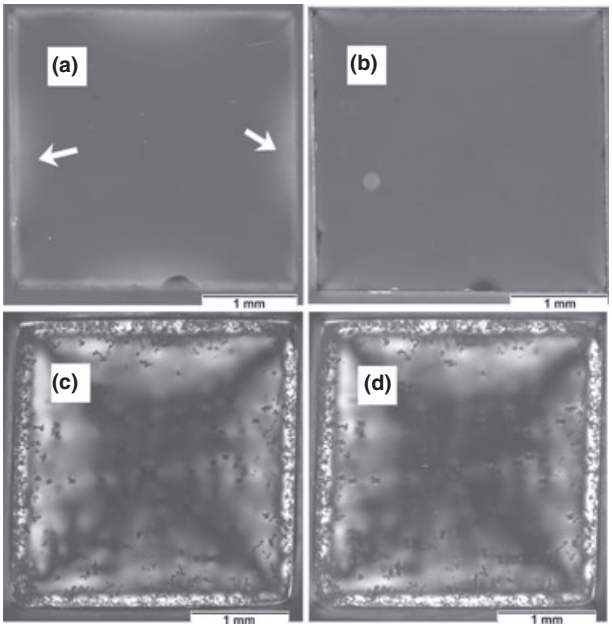

Fig. 7. Transmitted light optical micrographs of Br50 (0.17 at.% bromine) samples of cubic (~3 mm × 3 mm × 3 mm) shape. (a) 600°C for 5 min. (b) the same sample after annealing. (c) 600°C for 24 h. (d) the same sample after annealing. Cross-polarized contrast.

V. Conclusions

Bromine decreases the solubility of NaF in PTR glass, thus increasing the thermodynamic driving force for crystallization of NaF by increasing its super-saturation. This phenomenon limits the maximum volume fraction of crystallized NaF with decreasing the bromine content in the original glass. The glasses with lower bromine content reveal, after proper heat treatment, fewer crystals of a larger size, and dominant surface-initiated crystallization. Isothermal treatment of PTR glass at 600°C causes liquid–liquid phase separation with silica-enriched droplets, which decreases T_g because of increasing concentration of sodium and fluorine in the bulk glass. Conversely, NaF crystallization increases T_g because of decreasing the concentration of sodium and fluorine in bulk glass. The evolution of T_g as a function of isothermal treatment time revealed a minimum resulting from interplay between these two concurring processes. A surface layer of F-depleted glass results in residual stresses caused by the coefficient of thermal expansion mismatch between this layer and bulk glass. These stresses cannot be alleviated by annealing. The present results on the UV-unexposed glass should also be valid for the UV-exposed glass, but the kinetics of the transformations may be faster in the latter case due to the photo-induced process.

References

[1]V. A. Borgman, L. B. Glebov, N. V. Nikonorov, G. T. Petrovskii, V. V. Savvin, and A. D. Tsvetkov, "Photothermal Refractive Effect in Silicate Glasses," *Sov. Phys. Dokl.*, **34**, 1011–3 (1989).

[2]L. B. Glebov, "Photochromic and Photo-Thermo-Refractive Glasses"; pp. 770–80 in *Encyclopedia of Smart Materials*, Edited by Mel Schwartz. John Wiley & Sons, Inc., New York, 2002.

[3]O. M. Efimov, L. B. Glebov, and V. I. Smirnov, "High efficiency volume diffractive elements in photo-thermo-refractive glass"; Patent No. US 6,673,497 B2. January 6, 2004.

[4]L. B. Glebov, V. I. Smirnov, C. M. Stickley, and I. V. Ciapurin, "New Approach to Robust Optics for HEL Systems in Laser Weapons Technology III"; Edited byW. E. Tompson and P. H. Merritt, *Proceedings of SPIE*, **4724**, 101–9 (2002).

[5]S. D. Stookey, "Photosensitive Glass, a new Photographic Medium," *Ind. Eng. Chem.*, **41**, 856–61 (1949).

[6]T. Cardinal, O. M. Efimov, H. G. Francois-Saint-Cyr, L. B. Glebov, L. N. Glebova, and V. I. Smirnov, "Comparative Study of Photo-Induced Variations of X-ray Diffraction and Refractive Index in Photo-Thermo-Refractive Glass," *J. Non-Cryst. Solids*, **235**, 275–81 (2003).

[7]L. Glebova, J. Lumeau, M. Klimov, E. D. Zanotto, and L. B. Glebov, "Role of Bromine on the Thermal and Optical Properties of Photo-Thermo-Refractive Glass," *J. Non-Cryst. Solids*, **354**, 456–61 (2008).

[8]J. Lumeau, L. Glebova, G. P. Souza, E. D. Zanotto, and L. B. Glebov, "Effect of Cooling on the Optical Properties and Crystallization of UV-Exposed Photo-Thermo-Refractive Glass," *J. Non-Cryst. Solids*, **354**, 4730–6 (2008).

[9]G. P. Souza, V. M. Fokin, E. D. Zanotto, J. Lumeau, L. Glebova, and L. B. Glebov, "Micro and Nanostructures in Partially Crystallized Photothermo-refractive Glass," *Phys. Chem. Glasses Europ. J. Glass Sci. Technol. Part B*, **50** [5] 311–20 (2009).

[10]V. M. Fokin, G. P. Souza, E. D. Zanotto, J. Lumeau, L. Glebova, and L. B. Glebov, "Sodium Fluoride Solubility and Crystallization in Photo-Thermo-Refractive Glass," *J. Am. Ceram. Soc.*, **93** [3] 716–21 (2010).

[11]A. Monshi and P. F. Messer, "Ratio of Slopes Method for Quantitative X-ray-Diffraction Analysis," *J. Mater. Sci.*, **26** [13] 3623–7 (1991).

[12]J. Lumeau, A. Sinitskii, L. Glebova, L. B. Glebov, and E. D. Zanotto, "Method to Assess the Homogeneity of Partially Crystallized Glasses: Application to a Photo-Thermo-Refractive Glass," *J. Non-Cryst. Solids*, **355** [34–36] 1760–8 (2009).

[13]J. W. Christian, *The Theory of Transformations in Metals and Alloys*. Pergamon, London, 1965.

[14]G. P. Souza, V. M. Fokin, C. F. Rodrigues, A. C. M. Rodrigues, E. D. Zanotto, J. Lumeau, L. Glebova, and L. B. Glebov, "Liquid–Liquid Phase Separation in Photo-Thermo-Refractive Glass," *J. Am. Ceram. Soc.*, **94** [1] 86–91 (2011).

[15]J. H. Markis, K. Clemens, and M. Tomozawa, "Effect of Fluorine on the Phase Separation of Na_2O-SiO_2 Glasses," *J. Am. Ceram. Soc.*, **64** [1] C20 (1981). □